PROCEEDINGS, Thirty-Sixth Workshop on Geothermal Reservoir Engineering
Stanford University, Stanford, California, January 31 - February 2, 2011
SGP-TR-191

SUSTAINABLE HEAT FARMING OF GEOTHERMAL SYSTEMS: A CASE STUDY OF HEAT EXTRACTION AND THERMAL RECOVERY IN A MODEL EGS FRACTURED RESERVOIR

Daniel Sutter[1, 2], Don B. Fox[1], Brian J. Anderson[3], Donald L. Koch[4], Philipp Rudolf von Rohr[2], and Jefferson W. Tester[1,*]

[1]Atkinson Center for a Sustainable Future and the Cornell Energy Institute, Cornell University, Ithaca, NY 14853, USA
[2]Institute of Process Engineering, ETH Zurich, Sonneggstrasse 3, 8092 Zurich, Switzerland
[3]College of Engineering and Mineral Resources, West Virginia University, Morgantown, WV 26506, USA
[4]School of Chemical and Biomolecular Engineering, Cornell University, Ithaca, NY 14853, USA
[*]Corresponding author: jwt54@cornell.edu

ABSTRACT

To address the question of renewability of Enhanced Geothermal Systems (EGS) a conduction-dominated, model EGS reservoir was evaluated as a representative "worst case" to estimate heat extraction during production and thermal recovery following shut down. In the model system water is injected at specified rates and temperatures into a single rectangular fracture surrounded by an infinite amount of impermeable hot rock. During the extraction phase, water moves along the fracture extracting heat from the adjacent rock matrix leading to local cooling and thermal drawdown of the reservoir. When the water injection is stopped, conductive heat transfer from the surrounding hotter rock regions leads to thermal recovery of the cooler zones in the reservoir. The rate of recovery is controlled locally by the temperature gradient that is induced during the thermal drawdown. A two-dimensional mathematical model was developed to describe heat transfer for both extraction and recovery. Regarding the recovery, an advanced analytical approach was developed that is capable of describing the temperature during recovery at every position along the fracture. Our approach leads to the same result for the temperature at the inlet position, as presented in earlier research using a different approach. In addition, numerical simulations were carried out using the TOUGH2 code to study the importance of the assumptions employed in the analytical description and to extend the applicability of the model by enabling simulation of operating cycles with alternating extraction and recovery times. The effect of neglecting heat conduction in the rock in the direction parallel to the flow in the fracture was analyzed by comparison of the analytical model to the TOUGH2 simulations. For a fixed fracture area, low flow rates can result in thermal drawdown localized around the fluid inlet with heat conduction in the parallel direction becoming significant.

BACKGROUND AND MOTIVATION

One important feature of any operating geothermal reservoir system has to do with its anticipated production sustainability over the long term. Although geothermal reservoirs can be depleted during production if recharge rates are insufficient to overcome local cooling of rock and losses of fluid pressure, with proper management hydrothermal reservoirs have been shown to be productive for long periods of time. In Engineered Geothermal Systems the situation is different with no record of long term field testing and as a result the renewability of EGS in general is often questioned.

Axelsson et al. (2001) define the renewability of a geothermal source as the ability to maintain the installed capacity indefinitely. Thermally, the reservoir would be in steady-state condition, i.e. the rate of heat extraction by the working fluid and the recharge rate from the bulk rock are equal. However, the renewable capacity is frequently too small for commercial development due to economy of scale in infrastructure development and operation costs (Sanyal 2005). Therefore, considerations about the sustainability of geothermal systems must also include the recovery effect after a stop of heat extraction (Megel and Rybach 2000). Sanyal (2005) defines the sustainable capacity of a geothermal reservoir as the capacity, that can be economically maintained over the amortized life time of a power plant. According to his review of operating hydrothermal plants around the world, the sustainable capacity is 5 to 45 times the renewable capacity with the factor being most likely around 10. Although, exploiting the sustainable capacity eventually results in significant cooling of the reservoir and recovery times in the order of hundreds of years, there are good reasons to define such geothermal resource operation as sustainable.

- Complete recovery of the thermal energy is eventually guaranteed and even with recovery time

scales of hundreds of years the resource base is large enough to allow for long-term energy production (Tester, Anderson et al. 2006).

- The possible displacement of fossil fuel consumption would reduce environmental pollution today and help to preserve these fuels for future generations – as raw material and for possibly cleaner and more efficient power applications (Sanyal 2005).
- Geothermal resources can be considered renewable on time-scales of technological/societal systems, whereas fossil fuel reserves renew in geologic time scales only (Rybach, Megel et al. 2000).

Modeling the transient heat transfer in geothermal reservoirs allows studying different operating strategies with the overall goal to increase the sustainable capacity and make the best use of the heat flow from the surroundings that is induced by the extraction of heat.

The objective of this work is to model both operational modes of geothermal reservoirs: extraction and recovery phase. During the extraction phase, liquid water[1] is circulated through the reservoir under pressure to extract heat. During the recovery phase, the production flow is shut down and the heat flow from the surrounding rock recharges the reservoir. Both, a numerical and an analytical model to describe heat and mass transfer in the reservoir are developed. The results of both models are compared to each other for validation and to better understand the effect of some of the assumptions made in the analytical model.

THEORY

Analytical Model

The mathematical approach to the heat transfer problem is based on the model reservoir geometry given in Figure 1. The model system used for a discretely fractured EGS reservoir was adapted from earlier works by Gringarten et al. (1975) and Wunder and Murphy (1978). Although realistic reservoirs consist of a network of fractures, a single fracture model adequately captures thermal recovery through heat conduction from the hot rock surrounding the reservoir. A single rectangular, vertical fracture of constant width *2b* separates two blocks of homogeneous, isotropic, impermeable rock. A Cartesian coordinate system has been placed such that the *x=0* plane coincides with the rock/fracture interface.

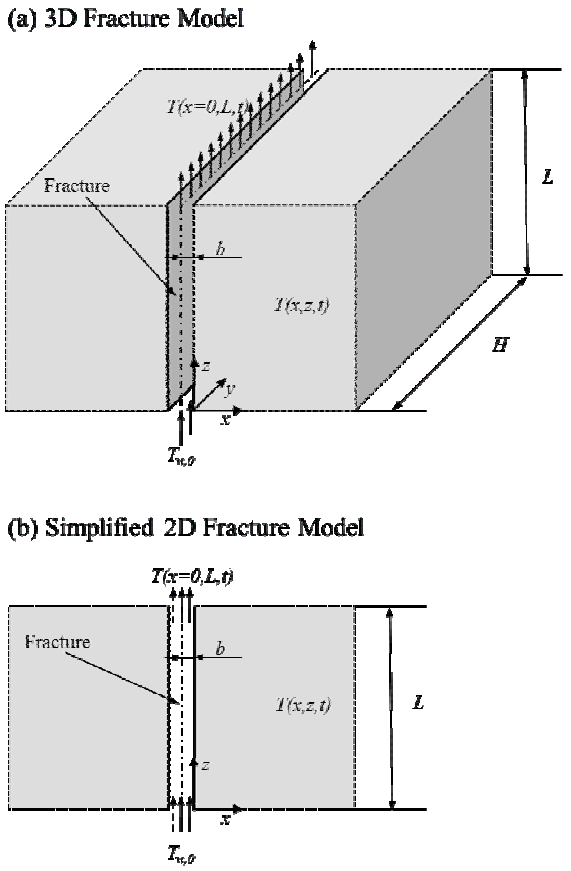

Figure 1: Mathematical model for single fracture in hot rock. (a) shows the three-dimensional model (3D), (b) shows the same model reduced to two dimensions (2D). The dashed line in the middle of the fracture indicates the symmetry in the x-direction.

The rock is assumed to extend horizontally (x) to infinity. Rock and fracture extend to infinity in the y-direction. Initially, ($t \leq 0$) the whole system is at uniform temperature $T_{r,0}$. For the heat extraction phase, water is injected at $x,z=0$ at a constant temperature $T_{w,0}$ and at a constant mass flow rate $\dot{m}$. It is flowing upwards through the fracture to the outlet at $x=0$ and $z=L$. Furthermore, the following assumptions are made:

- The temperature variation in the water in x-direction is insignificant, as the aperture of the fracture is very small compared to the fracture length ($b/L<<1$), and is neglected. For all z, the water temperature is equal to the rock temperature at $x=0$. In other words, the heat transfer resistance at the rock/water interface is neglected, which is a reasonable assumption for any practical case (Wunder and Murphy 1978; Ogino, Yamamura et al. 1999).
- Conduction in the vertical direction (z) in both the fracture and the rock formation is neglected, as

[1] In this report, we assume water to be the geothermal working fluid.

well as radiative heat transfer in the fracture. Because the aperture (*2b*) of the fracture in *x*-direction is small compared to the fracture extent in *y*-direction (*H*), such that *2b/H*<<1, we can extend the *y*-axis to $\pm\infty$ and neglect heat transfer in *y*. This effectively reduces the mathematical heat transfer problem to two spatial dimensions. Heat transfer occurs only by conduction in the rock in *x*-direction and forced convection along the *z*-direction in the fracture (Gringarten, Witherspoon et al. 1975).

- No heat flux occurs at the rock/fluid interface during recovery. The assumption is justified by the small volume, and hence, small heat capacity of the fracture compared to the volume/heat capacity of the rock that has been cooled during the preceding extraction phase.
- The density and specific heat capacity of both rock and water, and the heat conductivity of the rock are constant.
- The static fluid pressure in the fracture is set to exceed the vapor pressure of the water by a large enough margin to keep the fracture in single phase flow.

First extraction phase

The following derivation of a solution for the temperature field in a reservoir during the first extraction phase is based on the report of Wunder and Murphy (1978). A one-dimensional differential energy balance within the rock yields

$$\frac{\partial T}{\partial t} - \alpha \frac{\partial^2 T}{\partial x^2} = 0 \qquad (1)$$

where α is the rock thermal diffusivity, i.e. the ratio of thermal conductivity (k_r) and the product of density (ρ_r) and specific heat capacity ($c_{p,r}$)

$$\alpha = \frac{k_r}{\rho_r c_{p,r}} \qquad (2)$$

and $T=T(x,z,t)$ is the temperature. Following the assumptions of negligible heat transfer resistance at the rock/fluid interface and of negligible temperature variations in *x*-direction in the water, the temperature $T(x=0,z,t)$ describes the rock temperature at the interface and also the water temperature over the entire fracture width at the respective *z*-position. The temperature dependence on *z* is introduced in the boundary condition for the rock/fluid interface

$$\rho_w c_{p,w} b \frac{\partial T}{\partial t} + \rho_w c_{p,w} U b \frac{\partial T}{\partial z} = k_r \left.\frac{\partial T}{\partial x}\right|_{x=0} \qquad (3)$$

with *U* representing the flow velocity of the water, *b* the half-width of the fracture, and ρ_w and $c_{p,w}$ the density and specific heat capacity of the water. With the initial and bulk temperature of the rock specified as $T_{r,0}$ and the constant water temperature at the injection position taken as $T_{w,0}$ the additional boundary conditions are

$$T(x=0, z=0, t) = T_{w,0}\,, \quad t > 0 \qquad (4)$$

$$T(x \to \infty, z, t) = T_{r,0} \qquad (5)$$

and the initial condition is

$$T(x, z, t \le 0) = T_{r,0} \qquad (6)$$

The analytical solution is given in terms of the dimensionless, normalized temperature Θ and is based on the solution of a classical transient heat transfer problem as presented for example by Carslaw and Jaeger (1959) and Arpaci (1966)

$$\Theta(x, z, t) \equiv \frac{T(x, z, t) - T_{w,0}}{T_{r,0} - T_{w,0}} = erf\left[\frac{x + \beta z}{2\sqrt{\alpha t}}\right] \qquad (7)$$

where

$$\beta = \frac{k_r}{\rho_w c_{p,w} U b} \qquad (8)$$

First recovery phase

An advanced approach was developed to describe the temperature in the single fracture model analytically. We consider a linear heat sink along the fracture, i.e. in *z*-direction at $x=0$. Because of our earlier simplification to two dimensions, the sink appears at all *y* from $y=0$ to $y=H$. The line sink represents the heat extraction by the flowing fluid in the fracture during the extraction phase. The energy balance including the heat sink becomes

$$\frac{\partial T}{\partial t} - \alpha \frac{\partial^2 T}{\partial x^2} = \frac{q(z,t)\delta(x)}{\rho_r c_{p,r}} \qquad (9)$$

where $q(z,t)$ is the heat flux at the rock/water interface and $\delta(x)$ is the Dirac delta function. The discrepancy to Eq. (1) in the right hand side of the equation is resolved by noting that the boundary condition in Eq. (3) handles the heat sink in the previous formulation. As mentioned before, the temperature $T(x=0,z,t)$ is valid for both rock and water at the interface. The corresponding initial and boundary conditions of Eq. (9) are again Eq. (5) and Eq. (6). The heat flux $q(z,t)$ takes account of the second boundary condition.

During the extraction phase, heat flows from the hot regions of rock into the moving fluid in the fracture. The flux $q(z,t)$ can be determined based on the temperature profile for the extraction in Eq. (7). No heat flux occurs at the rock/water interface during the recovery phase, according to the assumption listed above, and $q(z,t)$ is then zero. With t_{ex} being the time at the end of the extraction phase and $u_0=T_{w,0}-T_{r,0}$, we get

$$q(z,t) = \begin{cases} -2k_r \left.\dfrac{\partial T}{\partial x}\right|_{x=0} = \dfrac{2k_r u_0}{\sqrt{\pi\alpha t}} \exp\left[-\dfrac{(\beta z)^2}{4\alpha t}\right], & 0 < t \le t_{ex} \\ 0, & t > t_{ex} \end{cases} \qquad (10)$$

Eq. (9) was solved using a variable transformation and the following Green's function (Duffy 2001)

$$G(x-x',t-t') = \frac{H(t-t')}{\sqrt{4\pi\alpha(t-t')}} \exp\left[\frac{-(x-x')^2}{4\alpha(t-t')}\right] \quad (11)$$

where *H(t-t')* is the Heaviside step function, which is equal to 1 for positive arguments and equal to 0 for negative arguments. For details on the derivation, see Appendix B. The solution in integral form is

$$\Theta(x,z,t) = 1 - \frac{1}{\pi}\int_0^{t_{ex}} \frac{H(t-t')}{\sqrt{t'}\sqrt{t-t'}} \exp\left[\frac{-1}{4\alpha}\left(\frac{x^2}{t-t'} + \frac{(\beta z)^2}{t'}\right)\right] dt' \quad (12)$$

Eq. (12) can be used for both extraction and recovery phase, i.e. for $t \in [0,\infty)$, if one extraction period with subsequent recovery is considered. For $t < t_{ex}$, the Heaviside step function *H(t–t')* effectively reduces the integration limits from $[0,t_{ex}]$ to $[0,t]$. The temperature at time $t = t_{ex}$ can be defined as the limit of Eq. (12) for $t \rightarrow t_{ex}$.

The integral in Eq. (12) has a closed form solution when $x,z=0$. The recovery solution ($t > t_{ex}$) at $x,z=0$ in terms of Θ is

$$\Theta(x=0,z=0,t) = \frac{2}{\pi}\tan^{-1}\left(\sqrt{\frac{t}{t_{ex}}-1}\right) \quad (13)$$

The same solution was reported by Wunder and Murphy (1978). They did not literally restrict the solution to the injection point at $x,z=0$ but assumed a "constant drawdown temperature" in their derivation. Nonetheless, in any practical situation the temperature during drawdown is constant only at the inlet position, where the fluid can be assumed to enter the system at a constant temperature.

Using Taylor series expansion and term wise integration, the integral can be solved analytically for $x=0$ and $z \in [0,L]$, i.e. for all positions along the fracture. For the derivation see Appendix B. The finally resulting infinite series is

$$\Theta(x=0,z,t) = 1 - \frac{1}{\pi}\sum_{n=0}^{\infty}\binom{n-\frac{1}{2}}{n}\left(\frac{t_{ex}}{t}\right)^{n+\frac{1}{2}} \times \left[\xi_r^{2n+1}\frac{(-1)^{n+1}2^{n+1}\sqrt{\pi}}{(2n+1)!!} erfc(\xi_r) + \exp\left(-\xi_r^2\right) \times \sum_{k=0}^{n}\frac{(-1)^k 2^{k+1}\xi_r^{2k}}{(2n+1)(2n-1)...(2n-2k+1)}\right], \; t > t_{ex}, \quad (14)$$

where $\xi_r = \frac{\beta z}{2\sqrt{\alpha t_{ex}}}$ and $\binom{n-\frac{1}{2}}{n}$ is a binomial coefficient. Eq. (14) only applies for the recovery phase and along the fracture, i.e. for $t > t_{ex}$ and $x=0$. Θ is minimal at the inlet and maximal at the outlet and the values can be used to obtain a range for the extent of the recovery of the geothermal reservoir. For example, when $\Theta = 1$ at the outlet, water could again be extracted at the initial rock temperature. If further time for recovery is specified, the *z*-position at which $\Theta = 1$ is reached, will retreat further towards the inlet, i.e. towards ($x=0$, $z=0$). When the recovery time becomes large compared to the extraction time, $t >> t_{ex}$, the heat sink due to the extraction fluid resembles an impulsive point source at $t=0$ and $x=0$. The first term of the infinite series in Eq. (14) is

$$\Theta_0 = 1 - \frac{2}{\pi}\left(\frac{t_{ex}}{t}\right)^{\frac{1}{2}}\left[\exp\left(-\xi_r^2\right) - \xi_r\sqrt{\pi}erfc(\xi_r)\right] \quad (15)$$

The same term can be found for an impulsive point source of magnitude

$$Q(z) = \int_0^{t_{ex}} q(z,t)dt = 4k_r u_0\left(\frac{t_{ex}}{\pi\alpha}\right)^{\frac{1}{2}}\left[\exp\left(-\xi_r^2\right) - \xi_r\sqrt{\pi}erfc(\xi_r)\right] \quad (16)$$

at $t=0$ and $x=0$.

Numerical Model

The TOUGH2 numerical simulator (Pruess, Oldenburg et al. 1999) was used for numerical modeling of extraction and recovery periods in the single-fracture system. TOUGH2 is a general purpose numerical simulation program for multi-dimensional non-isothermal flows of multi-phase, multi-component fluid mixtures in fractured and porous media. The code was developed at the Lawrence Berkeley National Laboratory and is written in standard FORTRAN77. It employs an integral finite difference method (IFDM) in discretizing the medium, which has the advantage of irregular discretization in multi-dimensions. Time is discretized fully implicitly as a first-order backward finite difference and fluxes are computed using upstream weighing (Pruess, Oldenburg et al. 1999).

PetraSim (Thunderhead Engineering, Manhattan, KS) was used as pre- and post-processing software at the front end. PetraSim allows to interactively define the mesh and parameters for the model and then creates an input file for the TOUGH2 code. After running the TOUGH2 code PetraSim can be used to process the simulation results for graphical representation.

Figure 2 shows a schematic view of the mesh applied for the numerical simulation in TOUGH2. Because of the symmetry along the *y*,*z*-plane in the middle of the fracture, only half of the basic model in Figure 1 was implemented. The simulated domain extends 300 m in *x*, 1 m in *y*, and 600 m in *z*. With a simple estimate for the penetration depth of the thermal cooling in the *x*-direction, $\Delta x = 2\sqrt{\alpha t}$, we find that 300 m will be reached after about 700 years only. The first column of gridblocks along the *z*-axis and at $x=0$ represents the fracture. The column of fracture cells and the first column of rock cells next to it are both 0.03 m wide. From there on, the mesh is logarithmically spaced into 18 more gridblocks in the *x*-direction. In the *z*-direction, the mesh is equally partitioned into 0.5 m

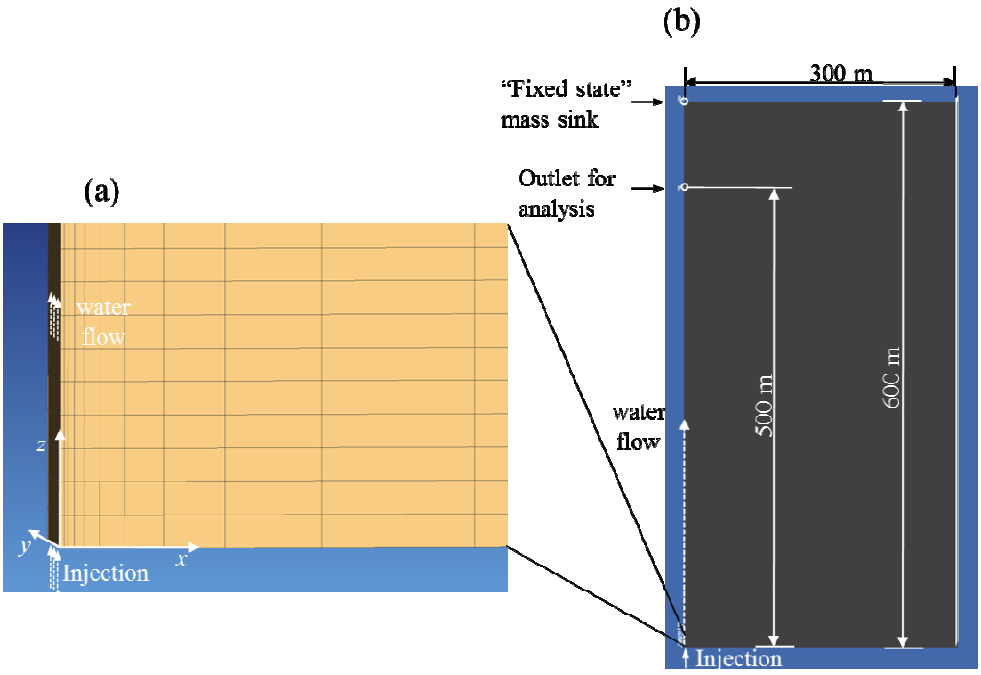

Figure 2: Mesh for TOUGH2 numerical simulation of a single fracture in hot rock. (b) shows the complete grid with dimensions and the positions of fluid injection and outlet. The model can be pictured as the right-hand half of the two dimensional system in Figure 1, Graph (a), including a two dimensional block of rock and half the fracture on its left-hand side. The lines indicating the mesh cause the model to appear homogeneously dark in this overall view. The detailed view in (a) shows the structure of the mesh around the injection position. The water flow occurs within the first column of cells which incorporate the 0.03 m wide fracture as schematically indicated in (a). Note that the extra cell with the source of mass does not appear in the figure.

blocks except near the inlet where the z-spacing was reduced to 0.25 m for the first ten meters from the injection point at x=0, z=0. The flow was assumed to be plug flow through the fracture; therefore, the mesh was not refined in the y-direction and consists of one layer of gridblocks in the x,z-plane. No heat and mass flow occurs at the boundaries at y=0 and y=1 m, and hence, no heat or mass flow can occur in the y-direction, the same as in the analytical model. The fracture cell at z=600 m is set to "fixed state" and represents a mass sink for the water flow along the fracture during the extraction phase. The "fixed state" specification keeps the cell's properties constant at their initial value, irrespective of occurring heat and mass exchange. However, the cell that is considered as the production well position in the analysis, is the fracture cell at z=L=500 m. The 100 m distance between the two cells was introduced to avoid undesirable effects from the "fixed state" cell definition on the spatial domain of interest of $z \in [0,L]$. An extra cell was added below the fracture cell at x,z=0 for the injection of fluid into the fracture. The extra cell includes a constant source of mass set to $\dot{m}$ representing the water injection. Pressure and enthalpy of the injected water have been specified to be 2 MPa and 85.275 kJ/kg, respectively, which corresponds to a temperature of $T_{w,0}$ = 20°C.

For the recovery phase, the mass source in the inlet cell is set to zero. The "fixed state" cell at the opposite end of the fracture at z=600 m is now enabled and set to the same initial temperature as the surrounding cells ("global initial conditions"). In order to limit the heat transfer from the surrounding rock to conduction, the porosity and permeability of the rock are set to 0. TOUGH2 includes only Darcy's Law flow models for porous media, so to model fluid flow in an open fracture, the porosity of the fracture material is set to 1.0, and its permeability to 10^{-9} m^2. While this is not a rigorous model of fluid flow in an open fracture and will not reproduce pressure drop accurately, the comparison with the theory which relies only on a specification of the flow rate in the crack will not be affected. A column of 0.001 m wide "fixed state" cells was added at the x=300 m boundary to achieve a constant temperature in the bulk rock. Pressure and temperature of this 21st column of cells in x are fixed at the initial conditions. All other boundaries of the mesh are inactive, i.e. no heat or mass flow occurs at the boundaries.

As given by (Armstead and Tester 1987) the drawdown rate of single fracture geothermal

reservoirs is determined by the parameter $\dot{m}/A$, the water mass flow rate $\dot{m}$ divided by the rock/water-interface area, $A=HL$. All flow rates in the discussion are given as "area-normalized" mass flows $\dot{m}/A$, which is equivalent to the thermal extraction rate per unit fracture area when multiplied by the heat capacity and temperature of the water. The magnitude of $\dot{m}/A$ scales directly with the rate of thermal drawdown.

RESULTS AND DISCUSSION

Figure 3 compares the results of the analytical extraction solution in Eq. (7) and the numerical simulation for the dimensionless, normalized temperature Θ at four different locations along the fracture. Analytical and numerical simulation results match closely for all positions. Generally, Θ decreases from its original value of 1 as heat is extracted from the system. At the inlet position (x,z=0) we see a sharp decline to $\Theta=0$, as required by the boundary condition in Eq. (4). For the reservoir and flow conditions specified (for a summary, see Appendix A), the temperature at the outlet (x=0, z=L=500 m) stays close to the initial temperature for the first 15 years. The penetration of the thermal cooling front along the fracture and into the rock in x-direction is discussed below.

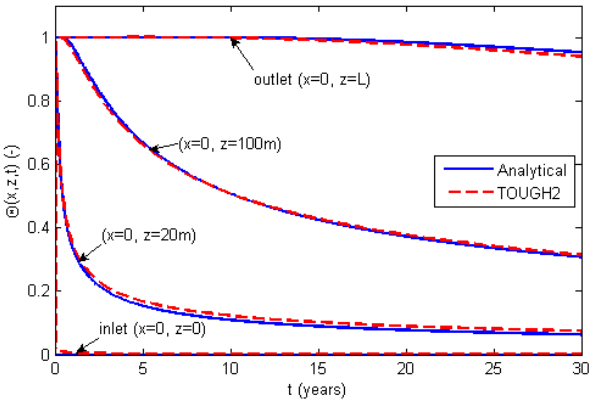

Figure 3: Comparison of the analytical solution for the extraction given in Eq. (7) and the TOUGH2 simulation result. The graphs show the normalized temperature Θ for a 30 years extraction period with an area-normalized water mass flow rate of $\dot{m}/A=8\times10^{-6}$ kg/(m^{2}s) ($U=1.33\times10^{-4}$ m/s) at four different locations along the fracture.

In order to verify the infinite series solution for the recovery phase in Eq. (14) it is compared to a numerical solution of the integral in Eq. (12) in Figure 4. The two solutions match well, when enough terms of the infinite series are considered. The time axis in Figure 4 and in the following illustrations of recovery is normalized by the extraction time t_{ex} and ranges from 1, the start of the recovery, to 6, where the time for recovery would be five times the duration of the extraction phase. The numerical integration solution will be used to compare the results of the analytical model and the TOUGH2 numerical model, because it allows to include positions in the rock matrix where $x\neq0$.

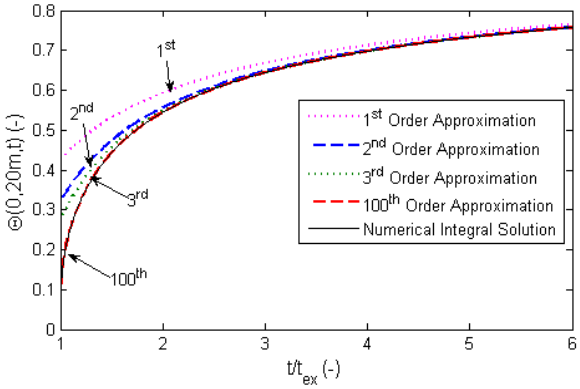

Figure 4: Trend of normalized temperature Θ at the position x=0, z=20 m with time during the recovery phase. The time axis is normalized by the extraction time t_{ex}. The continuous black line shows the solution obtained from the numerical integral solution, the dashed lines show the result of the analytical expression in Eq. (14) with an increasing number of terms of the infinite series being considered.

Figure 5 combines the results of the numerical integration solution and the TOUGH2 numerical simulation for the recovery phase at the four positions along the fracture introduced in Figure 3. The temperature in the TOUGH2 simulation exceeds

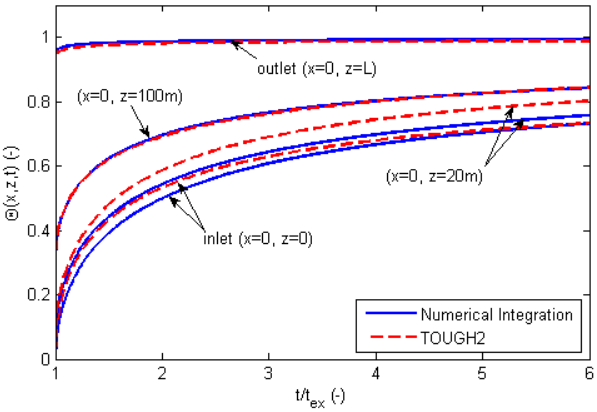

Figure 5: Results of the TOUGH2 simulation and the numerical integration for the recovery phase at four different positions along the fracture, after 30 years of heat extraction at an area-normalized water mass flow rate of $\dot{m}/A=8\times10^{-6}$ kg/(m^{2}s) ($U=1.33\times10^{-4}$ m/s).

the numerical integration solution for positions relatively close to the inlet, as can be seen for $x = 0$, $z = 20$ m in Figure 5. The absolute difference is $\Delta\Theta = 0.044$ at $t/t_{ex} = 6$.

A possible reason for the divergence is the different treatment of conduction heat transfer in the *z*-direction in the two models. The analytical solution is based on an energy balance that neglects conduction in *z* in the entire system, whereas the TOUGH2 model does consider conduction in *z*. Interestingly, the TOUGH2 solution results in faster thermal recovery. In order to investigate the importance of heat conduction in *z*, we compared analytical and TOUGH2 simulation results for a situation where the temperature gradients in the *z*-direction become negligible. Therefore, the area-normalized fluid mass flow rate for the extraction phase was increased to an artificially high value of $\dot{m}/A = 2\times10^{-3}$ kg/(m^{2}s), resulting in a temperature drawdown almost uniform in *z*, as shown in Figure 6.

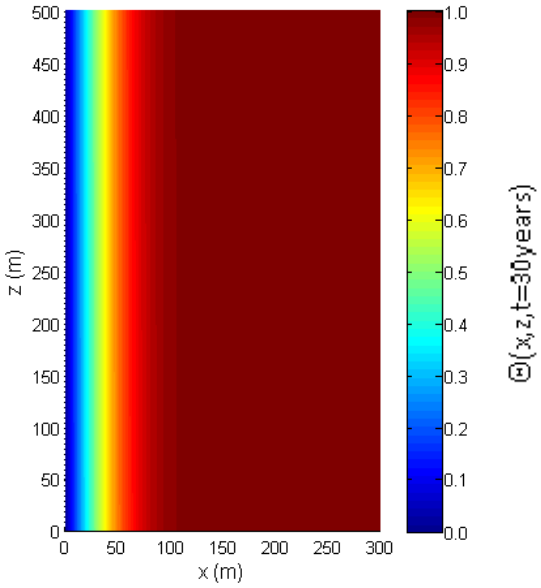

Figure 6: Temperature field after 30 year extraction period with an artificially high area-normalized water mass flow rate of $\dot{m}/A = 2\times10^{-3}\,kg/(m^2s)$ ($U = 3.33\times10^{-2}\,m/s$).

Indeed, the results of TOUGH2 and of the numerical integration solution match much closer for the thermal recovery from the temperature field with negligible gradients in the *z*-direction, as can be seen in Figure 7.

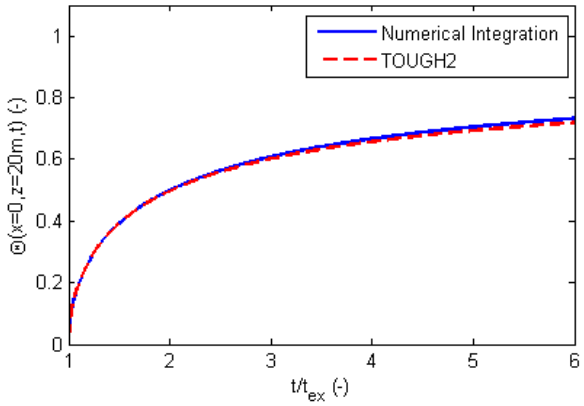

Figure 7: Results of the TOUGH2 simulation and the analytical solution for the recovery phase after a 30 year heat extraction phase at an area-normalized water mass flow rate of $\dot{m}/A = 2\times10^{-3}\,kg/(m^2s)$ ($U = 3.33\times10^{-2}\,m/s$) for the position x=0, z=20 m.

The same qualitative result was obtained for positions in the rock matrix at different distances from the fracture in *x*-direction. Figure 8 gives an example for the location 25 m into the rock and at the same distance to the inlet position in *z*-direction of 20 m. The applicability of the assumption of negligible heat conduction in the direction of the flow commonly made for the derivation of analytical solutions (Bodvarsson 1969; Gringarten, Witherspoon et al. 1975; Wunder and Murphy 1978; Bodvarsson and Tsang 1982; Cheng, Ghassemi et al. 2001) seems to be dependent on the flow rate of the extraction phase and the resulting temperature profile.

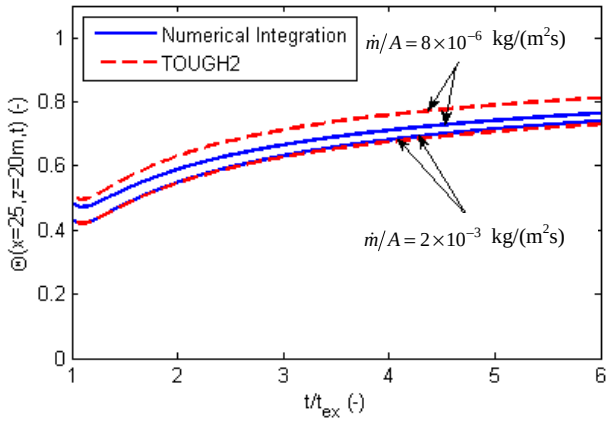

Figure 8: Results of the TOUGH2 simulation and the analytical solution for the recovery phase after a 30 year heat extraction phase at area-normalized water mass flow rates of $\dot{m}/A = 8\times10^{-6}\,kg/(m^2s)$ and $\dot{m}/A = 2\times10^{-3}\,kg/(m^2s)$ for the position x=25 m, z=20 m.

Conventional scaling analysis can be used to compare the order of magnitude of heat conduction in the two directions theoretically. The terms in the governing equation scale as

$$\frac{\partial^2 T}{\partial x^2} \sim \frac{\Delta T}{\delta_x^2} \tag{17}$$

$$\frac{\partial^2 T}{\partial z^2} \sim \frac{\Delta T}{\delta_z^2} \tag{18}$$

where ΔT, δ_x, and δ_z are the appropriate characteristic quantities for temperature and length in *x* and *z*, respectively. Hence, we can define a dimensionless quantity

$$\Lambda \equiv \frac{heat\ conduction\ \ in\ z}{heat\ conduction\ \ in\ x} \sim \left(\frac{\delta_x}{\delta_z}\right)^2 \tag{19}$$

In order to determine the relative importance of heat conduction along each axis, the characteristic length scale in both the *x*- and *z*-direction must be determined. δ_x and δ_z can be considered to be the penetration depth of the thermal cooling front along the *x*- and *z*-axis, respectively. Defining the position of the thermal cooling front to be the value of *x* or *z* at which Θ equals an arbitrary value ϑ, it can be described as

$$\Theta(\delta_x, 0, t) = \vartheta = erf\left[\frac{\delta_x}{2\sqrt{\alpha t}}\right] \tag{20}$$

$$\Theta(0, \delta_z, t) = \vartheta = erf\left[\frac{\beta\delta_z}{2\sqrt{\alpha t}}\right] \tag{21}$$

with β as defined in Eq. (8). Hence, our dimensionless quantity scales as follows

$$\Lambda \sim \beta^2 \propto \frac{1}{U^2} \propto \frac{1}{\dot{m}^2} \tag{22}$$

The numerical values for the two flow rates mentioned in this article are $\beta_1^2 \cong 3\times10^{-2}$ for the low flow rate and $\beta_2^2 \cong 5\times10^{-7}$ for the high flow rate. In other words, for the high flow rate heat conduction in *x* exceeds heat conduction in *z* by six orders of magnitude, while for the low flow rate the two become more comparable. For $\vartheta = 0.95$, the thermal penetration depths after the 30 year extraction phase at the lower flow rate corresponding to β_1 are $\delta_x = 86\,\text{m}$ and $\delta_z = 497\,\text{m}$, whereas for the high flow rate the theoretical penetration depth in *z* would be $\delta_z = 124'333\,\text{m}$. If we integrate thermal breakthrough to the fluid outlet position with its associated negative effects for the surface installation into our considerations, and thus restrict δ_z to L, we can conclude that the 1-D conduction model should be applied only for long fractures, where $\delta_x / L << 1$.

CONCLUSIONS AND OUTLOOK

The thermal behavior of a model fractured geothermal reservoir during heat extraction and thermal recovery was considered in this work. Firstly, a mathematical model was developed and solved analytically; secondly, numerical simulations were carried out to investigate the importance of the assumptions made in the analytical model and to extend the applicability of the single-fracture model to enable the numerical simulation of operation in extraction/recovery cycles.

The numerical model in combination with the analytical solutions was applied to investigate the importance of heat conduction in the rock matrix parallel to the fracture. The observed dependence on the area-normalized fluid flow rate could be confirmed quantitatively by a dimensionless parameter. Low area-normalized flow rates can result in thermal drawdown localized around the inlet position, and thus, create thermal gradients in the direction parallel to the fracture of comparable magnitude to the gradients in the direction orthogonal to the fracture. The most important specific findings are summarized below.

- An advanced approach was developed to describe the system mathematically with a linear heat sink along the fracture length being used to realize the heat extraction from the hot rock by the water flow through the fracture.
- A closed form analytical solution describing the temperature at the water inlet position during the recovery (and extraction) phase was derived. Although based on a different mathematical approach than used in an earlier study by Wunder and Murphy (1978), our solution for the recovery temperature at the inlet was consistent with that reported earlier.
- In addition, we developed an analytical solution for thermal recovery describing the temperature at all positions along the fracture. This more general infinite series solution allows to determine the temperature during the recovery phase at the position of the water outlet, for example. The outlet temperature is crucial as it corresponds directly to the production temperature of the geothermal fluid that would be utilized at the surface for generating power and/or providing heat.
- Using numerical integration, our analytical approach was successfully used to describe the transient thermal behavior of the entire spatial domain.
- Numerical simulation results from the developed TOUGH2 model and the analytical solution correspond closely for the tested range of different operating conditions and positions in the reservoir. This finding gives us confidence in modeling

drawdown and recovery scenarios for which analytical solutions are intractable.

- The developed dimensionless parameter can be applied to estimate the significance of two-dimensional conduction of heat. The one-dimensional simplification represents a lower bound for the temperature recovery in geothermal systems, as the additional conduction in the second dimension leads to faster recovery.

The model developed in the study can be used to evaluate strategies for the operation of geothermal reservoirs. Such strategies should aim at making the best use of the sustainable capacity of a given reservoir while guaranteeing the temperature requirements of the infrastructure at the surface. Among the operational scenarios to be tested are:

- Reservoir operation with several cycles, each consisting of one extraction and one recovery phase. Megel and Rybach (2000) compared operation scenarios with varying cycle durations while the overall extraction time and the mass flow rate during extraction were kept constant. They found that the overall extracted thermal energy increases with shorter cycle periods. Our model shows qualitatively consistent results. These basic results should be investigated in detail including different water mass flow rates and reservoir properties such as thermal conductivity of the rock. Different to Megel and Rybach (2000) we want to compare the overall exergy of the extracted hot fluid instead of its enthalpy.
- Graphical representations of the temperature in the modeled reservoir intuitively visualize how the reservoir implements a counter-current heat exchanger behavior when thermal breakthrough is reached. The temperature along the fracture gradually increases from $T_{w,0}$ at the fluid injection point to $T_{r,0}$ at the outlet. Before breakthrough is reached, the region close to the outlet position is inactive with respect to heat transfer from rock to water, because the water is already heated up to $T_{r,0}$ before it reaches the region. Contrary to the common notion that thermal breakthrough determines the termination of the reservoir usage, we want to explore ways how to use reservoirs that have seen breakthrough for preheating the geothermal fluid before it is transferred to a second reservoir. By this means one could make better use of the thermal energy in the first reservoir and simultaneously postpone breakthrough in the second reservoir, and hence, guarantee a constant production temperature of $T_{r,0}$ for much longer time.
- In order to increase the rock/water interface area, that is actively transferring heat to the fluid quickly, a higher flow rate at the beginning of the extraction phase could be advantageous. The flow rate should decrease later on to prevent early breakthrough. The effect on the total exergy that can be extracted from a reservoir needs to be investigated, along with strategies how to deal with the varying mass flow rate with respect to the surface installation.

REFERENCES

Armstead, H. C. H. and J. W. Tester (1987). Heat Mining. London, New York, E. & F.N. Spon.

Arpaci, V. S. (1966). Conduction Heat Transfer. Reading, Addison-Wesley.

Axelsson, G., A. Gudmundsson, et al. (2001). "Sustainable Production of Geothermal Energy: Suggested Definition." IGA-News 43(January-March): 1-2.

Bodvarsson, G. S. (1969). "On the Temperature of Water Flowing Through Fractures." Journal of Geophysical Research 74(8): 1987-1992.

Bodvarsson, G. S. and C. F. Tsang (1982). "Injection and Thermal Breakthrough in Fractured Geothermal Reservoirs." Journal of Geophysical Research 87(B2): 1031-1048.

Carslaw, H. S. and J. C. Jaeger (1959). Conduction of Heat in Solids. Oxford, Oxford University Press.

Cheng, A. H. D., A. Ghassemi, et al. (2001). "Integral Equation Solution of Heat Extraction from a Fracture in Hot Dry Rock." International Journal for Numerical and Analytical Methods in Geomechanics 25(13): 1327-1338.

Duffy, D. G. (2001). Green's Functions with Applications. Washington, D.C., Chapman & Hall/CRC.

Gradshteyn, I. S. and I. M. Ryzhik (2007). Table of Integrals, Series, and Products. New York, Academic Press.

Gringarten, A. C., P. A. Witherspoon, et al. (1975). "Theory of Heat Extraction from Fractured Hot Dry Rock." Journal of Geophysical Research 80(8): 1120-1124.

Megel, T. and L. Rybach (2000). Production Capacity and Sustainability of Geothermal Doublets. Proc. of the World Geothermal Congress, Kyushu - Tohoku, Japan.

Ogino, F., M. Yamamura, et al. (1999). "Heat transfer from hot dry rock to water flowing through a circular fracture." Geothermics 28(1): 21-44.

Pruess, K., C. Oldenburg, et al. (1999). TOUGH2 User's Guide, Version 2.0. Berkeley, CA, Lawrence Berkeley National Laboratory.

Rybach, L., T. Megel, et al. (2000). At What Time Scale are Geothermal Resources Renewable? Proc. of the World Geothermal Congress, Kyushu-Tohoku, Japan.

Sanyal, S. K. (2005). Sustainability and Renewability of Geothermal Power Capacity. Proc. of the World Geothermal Congress, Antalya, Turkey.

Tester, J. W., B. J. Anderson, et al. (2006). The Future of Geothermal Energy, Massachusetts Institute of Technology: 358.

Wunder, R. and H. Murphy (1978). Thermal Drawdown and Recovery of Singly and Multiply Fractured Hot Dry Rock Reservoirs. Los Alamos, New Mexico, Los Alamos Scientific Laboratory of the University of California.

APPENDIX

A. Nomenclature and Applied Numeric Values

$A = HL = 500$ m^2	rock/fracture interface
$\alpha = 1.023\times10^{-6}$ m^2/s	thermal diffusivity rock
$b = 0.03$ m	half-width of fracture
$\beta = \frac{k_r}{\rho_w c_{p,w} U b}$ (-)	dimensionless parameter
$c_{p,r} = 1050$ J/(kgK)	specific heat capacity rock
$c_{p,w} = 4184$ J/(kgK)	specific heat capacity water
δ_x, δ_z (m)	thermal penetration depth
$H = 1$ m	length of the model in *y* (TOUGH2)
$L = 500$ m	length of fracture in *z*
$\Lambda \sim \beta^2$ (-)	dim.less param. comparing conduction in *x* and *z*
$\dot{m}$ (kg/s)	water mass flow rate
$\dot{m}/A$ (kg/(m^{2}s))	area-normalized water mass flow rate
$k_r = 2.9$ W/(mK)	thermal conductivity rock
$k_w = 0.6$ W/(mK)	thermal conductivity water (TOUGH2)
$\rho_r = 2700$ kg/m^3	density rock
$\rho_w = 1000$ kg/m^3	density water
$T_{w,0} = 20°C$	water injection temperature
$T_{r,0} = 200°C$	initial rock temperature
$\Theta(x,z,t) \equiv \frac{T(x,z,t)-T_{w,0}}{T_{r,0}-T_{w,0}}$	dimensionless temperature
U (m/s)	water flow velocity
$\xi_r = \frac{\beta z}{2\sqrt{\alpha t_{ex}}}$	similarity variable for *x*=0, *t*=t_{ex}

B. Derivation for the Infinite Series Recovery Solution in Eq. (14)

We define a new variable which results in homogeneous boundary conditions and simplifies problem solving

$$u \equiv T(x,z,t) - T_{r,0} \tag{23}$$

Following the definition of Θ in Eq. (7) the relation of Θ and *u* is

$$\Theta = 1 - \frac{u}{u_0} \tag{24}$$

with u_0 defined as *u(x=0,z=0,t).* The transformations of Eq. (9) and its boundary and initial conditions in Eq. (5) and Eq. (6) are

$$\frac{\partial u}{\partial t} - \alpha \frac{\partial^2 u}{\partial x^2} = \frac{q(z,t)\delta(x)}{\rho_r c_{p,r}} \tag{25}$$

$$u(x,z,t \le 0) = 0 \tag{26}$$

$$u(x \to \infty, z, t) = 0 \tag{27}$$

The appropriate Green's function for the domain of $x \in \Re$ and $t \in \Re_0^+$ is shown in Eq. (11). Following the common approach for applying Green's functions the solution to the PDE in Eq. (25) is the integral

$$u(x,z,t) = \int_0^\infty \int_{-\infty}^\infty G(x-x', t-t') \frac{q(z,t')\delta(x')}{\rho_r c_{p,r}} dx' dt' \tag{28}$$

The dx' integral can be evaluated applying the sifting property of the delta function. The upper integration boundary for t' can be reduced from $t' = \infty$ to $t' = t_{ex}$, the time at the end of the extraction phase, because the heat flux *q(z,t)* is assumed to be 0 for the recovery phase ($t > t_{ex}$). The heat flux *q(z,t)* during the extraction phase can be determined applying the derivative of the temperature profile for the extraction in Eq. (7) as shown in Eq. (10). The result is

$$q(z,t) = \frac{2k_r u_0}{\sqrt{\pi \alpha t}} \exp\left[-\frac{\beta^2 z^2}{4\alpha t}\right], \quad 0 < t \le t_{ex} \tag{29}$$

Substituting the Green's function shown in Eq. (11) and the heat flux shown in Eq. (29) into Eq. (28) we get the general integral solution shown above in Eq. (12).

For $t > t_{ex}$, i.e. for the recovery period, Eq. (12) can be rewritten to be

$$\frac{u(x,z,t)}{u_0} = \frac{1}{\pi}\int_0^{t_{ex}} \frac{1}{\sqrt{t'}\sqrt{t}} \frac{1}{\sqrt{1-\frac{t'}{t}}} \exp\left[-\frac{1}{4\alpha}\left(\frac{x^2}{t-t'} + \frac{\beta^2 z^2}{t'}\right)\right] dt' \tag{30}$$

Using the Taylor series expansion for the term $\left(1-\frac{t'}{t}\right)^{-1/2}$ Eq. (30) can be simplified to

$$\frac{u(x,z,t)}{u_0} = \frac{1}{\pi^{n+1/2}} \sum_{n=0}^{\infty} \binom{n-\frac{1}{2}}{n} \int_0^{t_{ex}} t'^{n-1/2} \exp\left[-\frac{1}{4\alpha}\left(\frac{x^2}{t-t'} + \frac{\beta^2 z^2}{t'}\right)\right] dt' \tag{31}$$

For $x = 0$, the integral in each term of the summation in Eq. (31) can be expressed as an incomplete gamma function

$$\frac{u(x=0,z,t)}{u_0} = \frac{1}{\pi}\sum_{n=0}^{\infty}\binom{n-\frac{1}{2}}{n}\left(\frac{t_{ex}}{t}\right)^{n+1/2}\xi_r^{2n+1}\Gamma\left[-\left(n+\frac{1}{2}\right),\xi_r^2\right] \tag{32}$$

with ξ_r as defined below Eq. (14) and the incomplete gamma function defined as

$$\Gamma(a,s) = \int_s^{\infty}\tau^{a-1}e^{-\tau}\,d\tau \tag{33}$$

Applying the substitution $\tau = x^2$ the incomplete gamma function can be evaluated using the following integral found in Gradshteyn and Ryzhik (2007)

$$\int_v^{\infty}\frac{e^{-p^2x^2}}{x^{2m}}dx = \frac{(-1)^m 2^{m-1} p^{2m-1}\sqrt{\pi}}{(2m-1)!!}erfc(pv) + \frac{e^{-p^2v^2}}{2v^{2m-1}}\sum_{k=0}^{m-1}\frac{(-1)^k 2^{k+1}(pv)^{2k}}{(2m-1)(2m-3)...(2m-2k-1)}, \quad p>0 \tag{34}$$

and substituted in Eq. (32) to yield the infinite series solution given above in Eq. (14).